

# Fiber Bragg Grating Cavity Sensor for Simultaneous Measurement of Strain and Temperature

Wei-Chong Du, *Member, IEEE*, Xiao-Ming Tao, and Hwa-Yaw Tam, *Member, IEEE*

**Abstract**—A novel and short (5 mm long) fiber grating based sensor with a fiber grating Fabry–Perot cavity (GFPC) structure was fabricated and tested for simultaneous measurement of strain and temperature. The sensor exhibits unique properties that it possesses two spectral peaks within its main reflection band and the normalized peak power difference, in addition to its peak wavelength shift, changes linearly with strain or temperature. The accuracy of this particular sensor in measuring strain and temperature are estimated to be  $\pm 30 \mu\epsilon$  in a range from 0 to 3000  $\mu\epsilon$  and  $\pm 0.4^\circ\text{C}$  from 20  $^\circ\text{C}$  to 60  $^\circ\text{C}$ , respectively.

**Index Terms**—Fiber Bragg grating, FP cavity, simultaneous measurement of strain and temperature.

## I. INTRODUCTION

FIBER BRAGG gratings (FBG's) have emerged as powerful strain or temperature sensors [1]. However, temperature and strain cannot be determined separately by only measuring the wavelength shift of one FBG sensor, which is sensitive to both measurands. A number of techniques [2]–[6] have been reported to overcome this limitation. Most of them are based on the measurement of the different characteristic wavelength shifts of two types of gratings. It is highly desirable to use a single FBG sensor to encode strain and temperature into one more parameter, such as power or phase of the reflected light from the sensor. Recently, simultaneous measurement of dynamic strain and temperature using fiber Fabry–Perot (FFP) interferometer sensors was reported [7]. In this configuration, dynamic strain and temperature acting on the FFP are encoded as a change in their respective optical path difference and reflected wavelength. However, in this technique it is important to match the round-trip optical path length within the FFP interferometer to the imbalance of the Mach–Zehnder interferometer, which is 2 m long. Thus, the physical size of the sensor is very long (1 m), which may limit its use in some applications. This letter describe a novel and very short (5 mm long) fiber sensor based on an in-line Bragg grating Fabry–Perot cavity (GFPC). The spectral peak power of the reflected light from a GFPC sensor, in addition to its wavelength shift, varies linearly with strain or temperature.

Manuscript received July 7, 1998; revised September 14, 1998. This work was supported by the Hong Kong Polytechnic University.

W.-C. Du was with the South China Normal University and Hong Kong Polytechnic University. He is now with the R&D Department, MPB Communication, Inc., Pointe Claire, J9R IE9 Canada.

X.-M.Tao is with the Institute of Textile and Clothing, Hong Kong Polytechnic University, Kowloon, Hong Kong, China.

H.-Y. Tam is with the the Department of Electrical Engineering, Hong Kong Polytechnic University, Kowloon, Hong Kong, China.

Publisher Item Identifier S 1041-1135(99)00365-1.

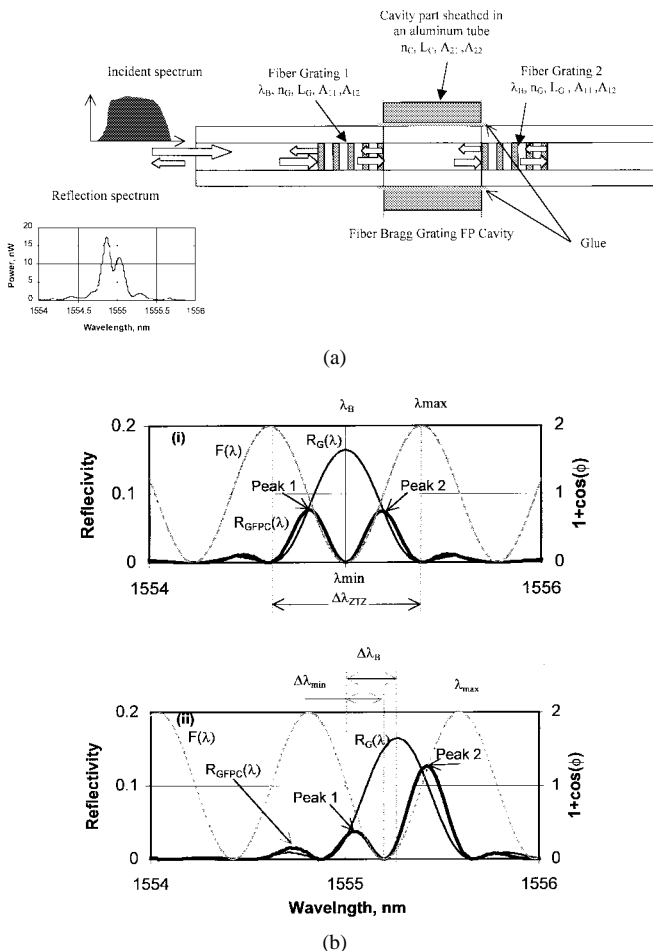


Fig. 1. (a) Structure of the novel grating Fabry–Perot cavity sensor and (b) calculated reflection spectrum of a GFPC sensor with the condition that (i)  $\lambda_B = \lambda_{\min}$  and (ii)  $\Delta\lambda_B > \Delta\lambda_{\min}$ .

Therefore, measurement of the peak wavelength shift as well as the change in the peak power of the light reflected from the sensor permits simultaneous determination of these two measurands.

## II. THEORY

The structure of a GFPC sensor is shown inserted in Fig. 1(a), which consists of two identical FBG's separated by a short cavity with a length of  $L_C$ . If the reflectivity of the two FBG's,  $R_G(\lambda)$ , is small, the reflection spectrum of the GFPC sensor,  $R_{GFPC}(\lambda)$ , is approximately given by

$$R_{GFPC}(\lambda) = CR_G(\lambda)F(\phi) \tag{1}$$

where  $C$  is a constant, and  $F(\phi) = 1 + \cos(\phi(\lambda))$ , is an interference function of the cavity and is determined by the phase difference ( $\phi(\lambda) = 4\pi n_C L_C / \lambda$ ) between the light reflected by the two gratings. The interference function can also be expressed as

$$F(\lambda) = 1 + \cos[4\pi n_C L_C / \lambda] \quad (2)$$

where  $n_C$  is the effective refractive index of the cavity section. Therefore, the reflection spectrum of the GFPC sensor is modulated by the cavity phase change. As a result, strain and temperature are encoded into the grating's Bragg wavelength shift and the variation in the cavity's phase difference or optical path. The change in the cavity's phase difference can be decoded by measuring the change in the total reflected power or the reflection spectrum profile of light from the sensor.

To illustrate this decoding principle, we plotted the spectra of  $R_G(\lambda)$ ,  $F(\lambda)$ , and  $R_{GFPC}(\lambda)$  of a GFPC sensor in Fig. 1(b). The grating's zero-to-zero reflection bandwidth ( $\Delta\lambda_{TZ}$ ) is approximately equal to one period of  $F(\phi)$  so that no more than two peaks appear in the GFPC main reflection band. When a minimum of  $F(\lambda)$  occurs within the grating's main reflection band, the GFPC reflection spectrum is split into two peaks, one on each side of the grating's Bragg wavelength ( $\lambda_B$ ). If this minimum,  $\lambda_{\min}$ , coincides with  $\lambda_B$  the intensity of the two peaks become equal and this is shown in Fig. 1(b(i)). With applied strain or temperature, both the grating's spectrum and the interference function as a result of change in phase difference vary. The respective shifts of  $\lambda_B$  and  $\lambda_{\min}$  can be expressed by

$$\begin{aligned} \frac{\Delta\lambda_B}{\lambda_B} &= A_{11}\Delta\varepsilon + A_{12}\Delta T \\ \frac{\Delta\lambda_{\min}}{\lambda_{\min}} &= A_{21}\Delta\varepsilon + A_{22}\Delta T \end{aligned} \quad (3)$$

where  $A_{i1}$  and  $A_{i2}$  are the strain and temperature coefficients of the grating ( $i = 1$ ) and cavity ( $i = 2$ ) sections, respectively. If the two sections have equal coefficients such that  $A_{11} = A_{21}$  and  $A_{12} = A_{22}$ , then the relative position between  $\lambda_{\min}$  and  $\lambda_B$  will not change with applied strain or temperature. In this case the reflection spectrum of the GFPC sensor shifts but its profile remains unchanged. Thus, temperature and strain can not be determined separately. However, if the grating and cavity sections have different strain and temperature coefficients. In the case that  $A_{11} > A_{21}$  or  $A_{12} > A_{22}$ ,  $\lambda_B$  will move at a faster rate than  $\lambda_{\min}$ . This results in a reduction in the intensity of peak 1 and an increase in the intensity of peak 2 when strain or temperature increases [Fig. 1(b(ii))]. When  $\lambda_B$  increases to coincide at the next maximum of  $F(\lambda)$  at  $\lambda_{\max}$ , peak 2 reaches a maximum value and peak 1 vanishes. Further increase in strain or temperature will result in two peaks in the GFPC reflection spectrum but in this case the intensity of peak 2 (corresponds to the longer wavelength) will decrease whereas, the intensity of peak 1 (corresponds to the shorter wavelength) increases. Therefore, the intensity of the two peaks changes periodically with strain and temperature.

The intensity fluctuation of the light source can be eliminated by introducing a normalized parameter  $M$ :

$$M = \frac{I_{P1} - I_{P2}}{I_{P1} + I_{P2}} \quad (4)$$

where  $I_{P1}$  and  $I_{P2}$  are the respective intensities of peaks 1 and 2.

Theoretically,  $M$  decreases (increases) monotonically from 1 to  $-1$  (from  $-1$  to 1) with strain or temperature when  $\lambda_B$  moves over one period from one maximum to the next maximum of the GFPC reflection spectrum. In practice, this range will be smaller because the reflection at the minimum of  $F(\lambda)$  is not zero and thus, the intensity of peaks 1 and 2 never becomes zero. In addition to the linear dependence of peak wavelength shifts upon strain and temperature, we now have a second relationship between  $M$  and strain or temperature of the GFPC sensor. If we assume this relationship is linear, then the two measurands can be determined simultaneously by measuring the changes in  $M$  and peak wavelengths follow by solving the linear matrix equation

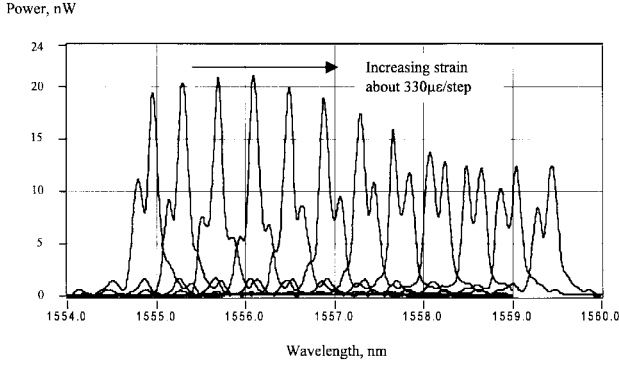
$$\begin{bmatrix} \Delta\lambda_p \\ \Delta M \end{bmatrix} = \begin{bmatrix} A'_{11} & A'_{12} \\ A'_{21} & A'_{22} \end{bmatrix} \begin{bmatrix} \Delta\varepsilon \\ \Delta T \end{bmatrix} \quad (5)$$

where  $\Delta\lambda_p$  is the wavelength shift of either peaks 1 or 2 with respect to strain or temperature. As we shall see in the next section that these two values are approximately equal.

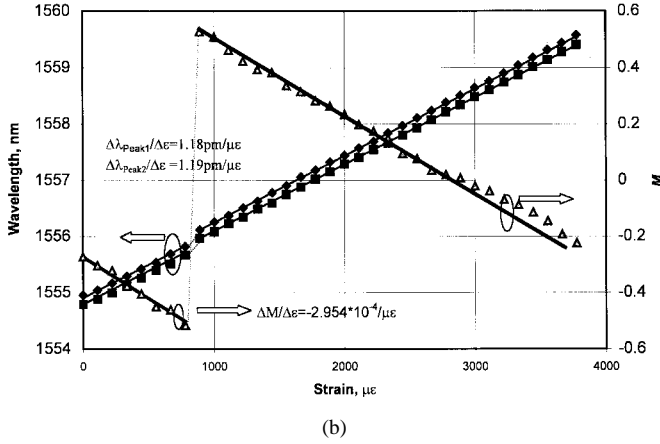
### III. EXPERIMENT AND RESULTS

The GFPC structure was written in a "hydrogen loaded" standard telecommunication single-mode fiber using a uniform phase mask (10 mm long) and a KrF<sub>2</sub> excimer laser. During the writing process, an aluminum plate with two parallel slits of 2 mm in width separated by 1 mm was placed between the phase mask and the laser beam (which has a dimension of 25 mm × 10 mm). In this way, two identical gratings of length 2 mm long, with their positions corresponding to that of the slits are written at the same time. The reflection spectra of the gratings and GFPC were measured with using an optical spectrum analyzer (OSA) with a resolution of 0.08 nm. The Bragg wavelength, zero-to-zero bandwidth, and central reflectivity of the two gratings are 1554.9 nm, 0.7 nm, and 10%, respectively. The cavity length is 1 mm long. Inserted in Fig. 1(a), a typical reflection spectrum of the GFPC sensor is illustrated. Two peaks can be observed in its main reflection band.

In order that the strain and temperature coefficients of the cavity section are different from those of the grating sections, a short (1 mm long) and thin aluminum tube (with an inside diameter of 0.3 mm and wall thickness of 0.15 mm) was glued onto the cavity section [shown as inserted Fig. 1(a)]. This section is now more difficult to stretch than the grating sections and thus its strain coefficient is correspondingly smaller so that  $A_{21} < A_{11}$ . On the other hand, its temperature coefficient becomes larger ( $A_{22} > A_{12}$ ). This is because the thermoexpansion coefficient of aluminum ( $23.5 \times 10^{-6}/^\circ\text{C}$ ) is much larger than that of the silica glass fiber, ( $0.5 \times 10^{-6}/^\circ\text{C}$ )



(a)



(b)

Fig. 2. (a) Measured reflection spectra of the GFPC sensor under different applied strain. (b) Relationship between  $M$ , peak wavelengths, and strain.

and expansion of the aluminum tube due to temperature rise induces additional strain to the cavity section.

We measured the strain and temperature coefficients of the GFPC sensor by independently applying strain and temperature to the sensor. Fig. 2 shows the result of an experiment in which the temperature was kept at 28 °C while the strain applied to the sensor was varied. It is clear from Fig. 2(a) that the two peaks vary sinusoidally as predicted in Section II. The wavelength shifts of peaks 1 and 2, and the normalized parameter  $M$ , calculated from the intensity of the two peaks, are plotted against the applied strain [Fig. 2(b)]. Discontinuity in the curves occur whenever  $\lambda_B$  coincides with a maximum in  $F(\lambda)$ . This in fact defines the range of  $M$ , which was measured to vary from  $-0.52$  to  $0.54$ . It can be seen that all three parameters vary linearly with strain and by fitting the experimental data using linear regression, we obtain

$$A'_{11} \approx \frac{\Delta\lambda_{P1}}{\Delta\varepsilon} = 1.18 \text{ pm}/\mu\varepsilon \approx \frac{\Delta\lambda_{P2}}{\Delta\varepsilon} = 1.19 \text{ pm}/\mu\varepsilon$$

$$A'_{21} = \frac{\Delta M}{\Delta\varepsilon} = -2.954 \times 10^{-4}/\mu\varepsilon.$$

Fig. 3 shows the experimental results for the determination of the temperature coefficients of the cavity and grating sections. Apart from the discontinuity around 61 °C, all three parameters vary linearly with temperature. However,  $M$  becomes nonlinear at temperature above 87 °C. This is most likely due to the glue whose operating temperature is not

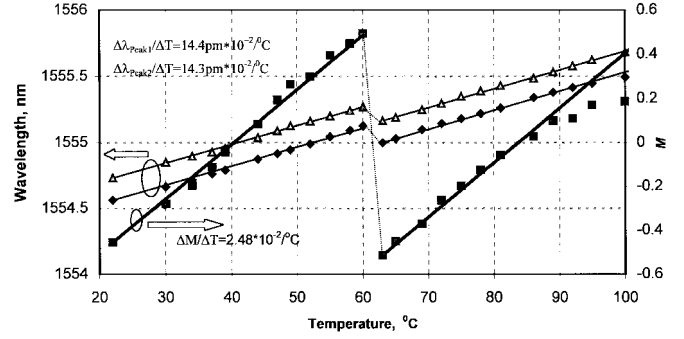


Fig. 3. Relationship between  $M$ , peak wavelengths on temperature.

known. From the slopes of these curves, we obtain

$$A'_{12} = \frac{\Delta\lambda_p}{\Delta T} \approx 14.35 \text{ pm}/^\circ\text{C}$$

$$A'_{22} = \frac{\Delta M}{\Delta T} = 2.48 \times 10^{-2}/^\circ\text{C}.$$

Therefore, by inserting the value of these coefficients into (5), strain and temperature can be calculated from the wavelength shift and intensity change measured by the GFPC sensor. From Figs. 2(b) and 3, the accuracy of this particular sensor in measuring strain and temperature are estimated to be  $\pm 30 \mu\varepsilon$  in a strain range of from 0 to 3000  $\mu\varepsilon$  and an  $\pm 0.4$  °C in a temperature range of from 20 °C to 60 °C, respectively.

These preliminary results have demonstrated that the sensor could perform simultaneous measurement of strain and temperature. It is important to note that the discontinuity point can be moved out of the measurement range by optimizing the lengths of the cavity and grating sections or by using different materials to glue the cavity section for varying  $A_{21}$  and  $A_{22}$ . The measurement range can be extended similarly by optimizing these parameters.

In conclusion, we have reported the operation and preliminary experimental results of a novel GFPC sensor for simultaneous measurement of strain and temperature.

## REFERENCES

- [1] A. D. Kersey, M. A. Davis, H. J. Patrick, M. LeBlanc, K. P. Koo, C. G. Askins, M. A. Putnam, and E. J. Friebele, "Fiber grating sensor," *J. Lightwave Technol.*, vol. 15, pp. 1442–1463, 1997.
- [2] A. D. Kersey, T. A. Berkoff, and W. W. Morey, "Fiber optic Bragg grating strain sensor with drift compensated high resolution interferometric wavelength shift detection," *Opt. Lett.*, vol. 18, pp. 72–74, 1993.
- [3] M. Xu, J. L. Archambault, L. Reekie, and J. P. Dakin, "Discrimination between strain and temperature effect using dual wavelength fiber grating sensors," *Electron. Lett.*, vol. 30, pp. 1085–1087, 1994.
- [4] H. J. Patrick, G. M. Williams, A. D. Kersey, J. R. Pedrazzani, and A. M. Vengsarkar, "Hybrid fiber Bragg grating/long period fiber grating sensor for strain/temperature discrimination," *IEEE Photon. Technol. Lett.*, vol. 8, pp. 1223–1225, 1996.
- [5] S. E. Kanellopoulos, V. A. Handerek, and A. J. Rogers, "Simultaneous strain and temperature sensing with photogenerated in-fiber gratings," *Opt. Lett.*, vol. 20, pp. 333–335, 1995.
- [6] S. W. James, M. L. Dockney, and R. P. Tatam, "Simultaneous independent temperature and strain measurement using in-fiber Bragg grating sensors," *Electron. Lett.*, vol. 32, pp. 1133–1134, 1996.
- [7] P. J. Henderson, Y. J. Rao, D. A. Jackson, J. Zhang, and I. Ben-El-Mechaieq, "Simultaneous dynamic-strain and temperature monitoring using a wavelength-multiplex fiber Fabry-Perot array with low-coherence interrogation," in *Proc. OFS'12*, Williamsburg, VA, Oct. 1997, pp. 56–59.